

Osteogenic differentiation of mesenchymal stem cells on random and aligned PAN/PPy nanofibrous scaffolds

Atike Ince Yardimci , Oznur Baskan, Selahattin Yilmaz, Gulistan Mese, Engin Ozcivici and Yusuf Selamet

Abstract

The aim of this study was to develop random and aligned polyacrylonitrile (PAN)/polypyrrole (PPy) nanofibrous scaffolds by electrospinning technique for osteogenic differentiation of mesenchymal stem cells. Nanofibers were fabricated successfully as straight, smooth, and free from bead formation. The average diameter of random and aligned nanofibers was $268(\pm 49)$ nm and $225(\pm 72)$ nm, respectively. Alignment process increased the tensile strength of nanofibers 3.9-fold, while the tensile strain of nanofibers decreased by 78%. PAN/PPy nanofibers were hydrophilic with the contact angle value of about 32° and alignment did not affect the contact angle value. Random and aligned PAN/PPy nanofibers were investigated as a scaffold material for osteogenic differentiation of DI ORL UVA mouse bone marrow mesenchymal stem cells. Cells were able to attach and grow on nanofibers confirmed by cell viability results. Stem cells that were cultured with osteogenic induction were able to mineralize on electrospun nanofibers based on alizarin red and Von Kossa dye staining. For aligned PPy nanofibers, mineralization occurred in the fiber alignment direction. Consequently, PAN/PPy nanofibrous mats in both random and aligned forms would be potential candidates for bone tissue engineering.

Keywords

Nanofiber, electrospinning, polypyrrole, mesenchymal stem cell, osteogenic differentiation

Introduction

Tissue engineering is a fast-growing field, which utilizes a combination of scaffolds, cells, and biologically active molecules to improve or restore anatomical and physiological functions.¹ Biological tissues are characterized by their mechanical, chemical, and morphological properties that are mainly governed by extracellular matrix (ECM) proteins of that tissue. The main goal of tissue engineered scaffolds is to mimic the ECM for cells that are aimed to be grown, and most scaffolds are fabricated from polymers via various methods such as solvent casting and particulate leaching, melt molding, rapid prototyping, phase separation, and electrospinning.² Among these methods, electrospinning provides nanofibers with excellent interconnectivity,³ and porosity for the integration of cells into the scaffold with an appropriate pore size.^{4–7} Therefore, electrospun polymer nanofibers became a frequently used tool in tissue engineering^{3,8–10} and drug delivery^{11–14} applications.

Electrospun nanofibrous scaffolds can be engineered to closely mimic the ECM based on their tunable

mechanical, chemical, degradative, and surface properties.¹⁵ Various scaffold types for biomedical applications spanning from nerve to bone tissue engineering can be studied with electrospinning methodology based on the versatility in its nature.⁵ An important aspect that governs the mechanical properties of various tissues including skeletal muscle, nerve, and vasculature is their anisotropic structure. These tissues show high elasticity in the direction of their extracellular matrix fibers alignment.¹⁶ The fabrication methodology of electrospun nanofibers can easily be extended to align fibers during the collection process leading to the formation of

Material Science and Engineering Department, Izmir Institute of Technology – Gulbahce Campus, Urla, Turkey

Corresponding author:

Atike Ince Yardimci, Material Science and Engineering Department, Izmir Institute of Technology – Gulbahce Campus, Urla, Izmir 35430, Turkey.
Email: atikeince@gmail.com

aligned structures that promote the growth of cells neural, muscle, and spinal disc applications.^{17–19}

Bone tissue is also known to be anisotropic.^{20,21} It is therefore not surprising that several studies investigated effects of aligned synthetic or natural polymer electrospun fibers in bone tissue engineering applications.^{22–24} In essence, aligned fibers enable bone cell growth and alignment in the fiber directions. However, to date none of these studies used a biocompatible conductive polymer. Finally, it is currently not known whether aligned fibers also facilitate calcification in the direction of alignment for bone cells.

For this study, we used polypyrrole (PPy), which is a conductive polymer with known biocompatibility.^{25–31} PPy is nontoxic and thin films made of PPy support attachment, adhesion, and the osteogenic differentiation of mesenchymal stem cells as well.³² Here, we developed 3D polyacrylonitrile (PAN)/PPy scaffolds by an electrospinning method and tested for osteogenic differentiation of mesenchymal stem cells. It was observed that these nanofibers supported attachment, proliferation, and differentiation of mesenchymal stem cells. In addition, nanofiber alignment governed the direction of mineralization during osteogenesis, showing that PAN/PPy conductive scaffold is a potential candidate for bone tissue applications.

Materials and methods

PAN/PPy solutions preparation and electrospinning

In order to synthesize PAN/PPy scaffolds, electrospinning method was used. We used PPy with PAN as a co-polymer during electrospinning process as PAN enhances the solubility of PPy.³³ In order to prepare electrospinning solution, first 8 wt% PAN was dissolved in DMF until a clear solution was obtained by mechanical stirring, then PPy was added to the solution with 10 wt% concentration of the total polymer mass. These PAN/PPy solutions were prepared with mechanical stirring for minimum 72 h at 60°C.

Obtained solutions were loaded to a 5 mL syringe connected to a high voltage of 15 kV for the electrospinning process. Solution flow rate was kept at 1.5 mL/h and the distance between the syringe and collector was 20 cm. The fibers were collected on 10 mm diameter coverslips, which were fixed on Al foil. Random and aligned nanofibers were collected on a drum collector with dimensions of 10 cm in diameter and 25 cm in length. Rotation speed to synthesize nanofibers was set to 250 r/min for random orientation and 1000 r/min for aligned orientation.

Nanofibers characterization

The morphology and diameter of PAN/PPy nanofibers were analyzed by scanning electron microscope (SEM) (FEI QUANTA 250 FEG). Tensile tests of nanofibers were carried out with a 5 kg load cell under 0.1 mm/s test speed (TA.XT plus texture analyzer). For tensile tests, sample dimensions were kept as 8 mm × 60 mm. The wettability of PAN/PPy electrospun nanofibers was analyzed by water contact angle measurement test (Attention-Theta analysis system). The droplet size was 3 μ L and at least five readings were taken for each sample. To examine the changes in the molecular orientation, random and aligned PAN/PPy nanofibers were analyzed with Fourier-transform infrared spectroscopy (FT-IR) (Perkin Elmer) with a wire grid polarizer with 4 cm^{-1} resolution. In parallel/perpendicular polarization, the direction of oscillating electric field of the IR beam was parallel/perpendicular to the alignment direction of nanofibers. Cyclic voltammetry (CV) and electrochemical impedance spectroscopy (EIS) methods were utilized for electrochemical measurements of the PAN/PPy nanofibers. A three-electrode electrochemical cell including a graphite working electrode covered with the nanofibers during electrospinning process, an Ag/AgCl reference electrode and a Pt wire counter electrode was used for both techniques. The electrolyte solution was 0.1 M HCl solution for CV and Fe[CN6]3-/4 solution for EIS. The EIS graphs of the nanofibers were taken in the frequency range of 0.01 Hz to 100 kHz.

Osteogenic differentiation of mesenchymal stem cells on PAN/PPy nanofibrous scaffold

In this study, D1 ORL UVA (ATCC) bone marrow stem cells were used as a biological model.³⁴ PAN/PPy nanofibers on coverslips were sterilized by incubation at 200°C for 3 h and then cells were seeded on nanofibers in 24-well cell culture plates at 500 cell/well density. Cells were grown until day 7, 14, and 21 for morphological assessment by SEM and viability assessment by MTT assay. D1 ORL UVA mesenchymal stem cells were either grown quiescent (DMEM + 10% FBS + 2% Pen/Strep) or induced 50% and 100% osteogenic medium. Two different osteogenic medium was tried with different contents: first tried osteogenic media was quiescent media + 10 nM β -glycerolphosphate and 50 μ g/mL ascorbic acid³⁵ and the second was quiescent media + 10 nM β -glycerolphosphate + 50 μ g/mL ascorbic acid and 10 nM dexamethasone.

Characterization of cells

After 7, 14, and 21 days of culture, morphology of cells were analyzed with SEM. Cells were washed with

phosphate-buffered saline (PBS) and then fixed with 4% paraformaldehyde for 3–4 h at room temperature. After fixation, cells were washed with PBS and ultra-pure water and then air dried. Dry cellular constructs were sputter coated with gold and observed under the SEM at an accelerating voltage of 5 kV.

Cell viability was determined by MTT (3-(4,5-Dimethylthiazol-2-yl)-2,5-diphenyltetrazolium bromide) assay. Culture medium was replaced with 10% MTT solution containing medium and the plates were incubated at 37°C, 5% CO₂ for 4 h. During the incubation, the active enzymes of the viable cells transformed the yellow MTT into purple formazan crystals. The top medium was then removed and DMSO was added to each well to dissolve the formazan crystals. The absorbance of the solution was measured at 570 nm and 650 nm (Thermo Multiskan).

Presence of calcified matrix on PAN/PPy electrospun nanofibers was detected with Alizarin red and von Kossa staining at 21 days of quiescent or osteogenic culture of DI ORL UVA cells. Cells were first washed with 1 mL of PBS (×3) and then fixed with 500 μL of 10% neutral buffered formalin for 30 min. Afterwards, cells were washed again (×2) with 1 mL of deionized (DI) water and stained with 1 mL of Alizarin red dye for 30 min. After staining, cells were rinsed (×2) with DI water, and washed in PBS for 15 min to remove nonspecific binding of dye. Micrographs of calcified matrix were taken through the light field of an inverted microscope (Olympus, IX-83).

For von Kossa staining firstly cells were fixed with 4% PFA for 20 min. Subsequently, PBS was discarded on the cells fixed in tissue culture plate and rinsed with DI water. One mL of a 1% silver nitrate solution was added and the plate was placed under UV light in laminar flow for 30 min. After incubation, cells were rinsed

in DI water several times. Then, to remove unreacted silver 500 μL of 5% sodium thiosulfate was put and incubated for 5 min. Lastly, cells were rinsed with DI water again and kept the water inside the wells until observation under light microscope.

Statistics

All results were reported as mean ± standard deviation. Statistical comparisons were made by Student's t-test in excel.

Results and discussions

Alignment of nanofibers in electrospinning method requires high rotation speed, usually 1000 r/min or higher speeds.^{36,37} In this study, PAN/PPy nanofibers were electrospun in different spinning velocities that resulted in either random (with 250 r/min) or aligned (1000 r/min) orientations (Figure 1). Physical comparison of aligned and random nanofibers yields similar fiber diameters (Table 1). Contact angle measurements also displayed similar hydrophilicity (~32°) for both PAN/PPy random and oriented setups ($p < 0.05$), a result that is clearly distinct from a pure PPy, which is hydrophobic in nature (Table 1). Increased hydrophilicity of polymers is essential for using them in tissue culture applications, as cells tend to favor hydrophilic surfaces for attachment, migration and growth.³⁸ Alignment of PAN/PPy nanofibers also affected bulk mechanical properties by increasing tensile strength 3.9-fold ($p < 0.01$), and decreasing tensile strain 78% ($p = 0.01$) (Table 1). Our results indicated that mechanical properties of nanofiber scaffolds are highly dependent on the orientation distribution of the nanofibers and oriented scaffolds can resist high tensile loads on the alignment axis relative to random scaffolds

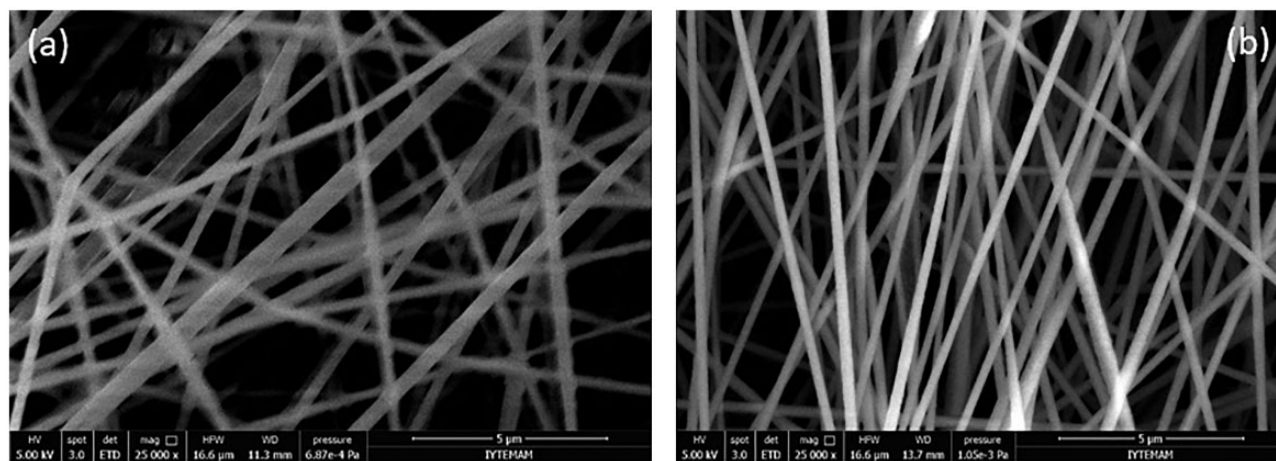
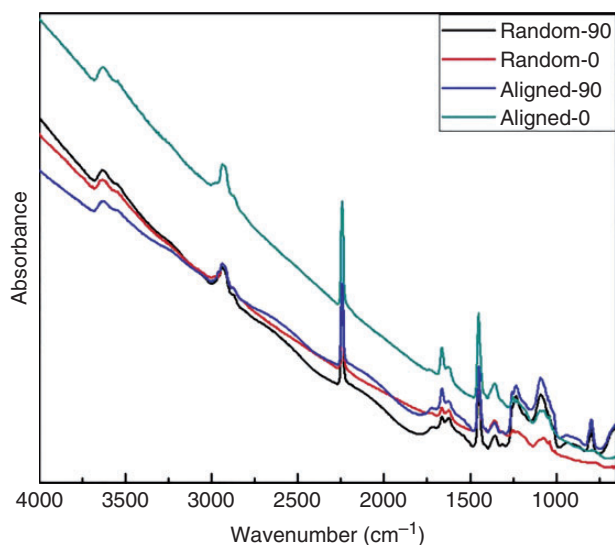


Figure 1. SEM images of (a) random (b) aligned PAN/PPy nanofibers at 5 μm scale.

Table 1. Average diameter, tensile properties and contact angles of random and aligned PAN/PPy nanofibers (NFs) containing 10 wt% PPy.

Nanofibers	Average diameter (nm)	Tensile strain (%)	Tensile strength (MPa)	Contact angle (°)
Random NFs	268 (± 49)	23.33 (± 3.17)	9.34 (± 1.3)	32.817 (± 1.54)
Aligned NFs	225 (± 72)	5.15 (± 1.87)	36.77 (± 2.1)	32.005 (± 1.24)

**Figure 2.** Polarized FT-IR spectra (parallel (0°) and perpendicular (90°) polarized IR spectra) of random and aligned PAN/PPy nanofibers.

consistent with literature.^{39–41} Mechanical strain has a significant influence in growth and development of osteoblasts and bone tissue^{42,43} and promotes matrix mineralization of osteoblasts.^{44,45}

Polarized FT-IR spectra of the random and aligned PAN/PPy nanofibers were performed for confirmation of fiber alignment (Figure 2). The peaks at 1270 cm^{-1} and 1654 cm^{-1} are induced by C-N and C=N stretching, respectively. The peaks observed at 1454 cm^{-1} and 2237 cm^{-1} were the characteristics vibrations peaks of PAN.³³ FT-IR results confirmed the PPy existence in PAN solution. For random nanofibers, positions and peak intensities of parallel and perpendicularly polarized FT-IR spectra were the same indicating that there was no specific molecular orientation in this sample. When the IR beam was polarized parallel to the fiber axis (green line), higher absorption was observed. The intensities and peak positions were changed for parallel and perpendicular directions. FT-IR spectroscopy relays structural information on oriented and ordered molecules. Molecular orientation occurring during various forming processes significantly affects mechanical properties of polymers, therefore, to determine the molecular mechanism of polymer deformation, the

measurement of this orientation is significant. For a polymer sample, the differences in band intensities between parallel and perpendicular polarized infrared spectra demonstrate high degree of orientation of the polymer chains while similar band intensities between parallel and perpendicular polarized infrared spectra mean random orientation with little order. The quantitative relationship between the preferred orientation and fiber morphology was reported in literature.^{46,47} The polarized FT-IR spectra of aligned PAN/PPy nanofibers showed anisotropy, indicating that the polymer chain in the fiber was stretched and aligned in the fiber axis during electrospinning process.

PAN/PPy nanofibers cyclic voltammetry (CV) results showed two oxidation peaks at 0.2 and 0.7 V and two reduction peaks at 0.1 and 0.45 V (Figure 3). CV results of the fibers indicated that these nanofibers were electroactive and can be used as an electrochemical actuator in acidic solutions. The electrode/electrolyte interfacial resistance of PAN/PPy as obtained through Nyquist plots displayed semicircles with a diameter at the intermediate frequency region representing the charge-transfer resistance of nanofibers (Figure 3(b)). Average impedance value of the nanofibers calculated from Nyquist plots was $1245\ \Omega$. PPy existence decreased the resistance value, and provided conductive nanofibers.⁴⁸ Porous structure of nanofibers and the high affinity of PAN and PPy to the liquid electrolyte contribute to low interfacial resistances.⁴⁹

SEM images illustrated randomly distributed D1 ORL UVA mesenchymal stem cells on two dimensional glass surface (Figure 4). D1 cells attached and spread on glass in both growth medium (GM) and osteogenic medium (OM). Consistent with the literature,³⁵ D1 cells that were cultured in OM for 21 days showed mineralization. D1 cells were able to attach randomly oriented PAN/PPy nanofibers for both growth and osteogenic conditions as evidenced by SEM images (Figure 5). Cells formed intimate contact with multiple fibers and displayed rough topography. D1 cells, that normally form extremely packed colonies in the absence of an ECM,⁵⁰ initially formed distinct colonies but after three weeks of culture, they covered the whole surface of nanofibers and mineralization was observed for cells that were grown in osteogenic conditions. D1 cells that were cultured on aligned PAN/PPy nanofibers, depicted

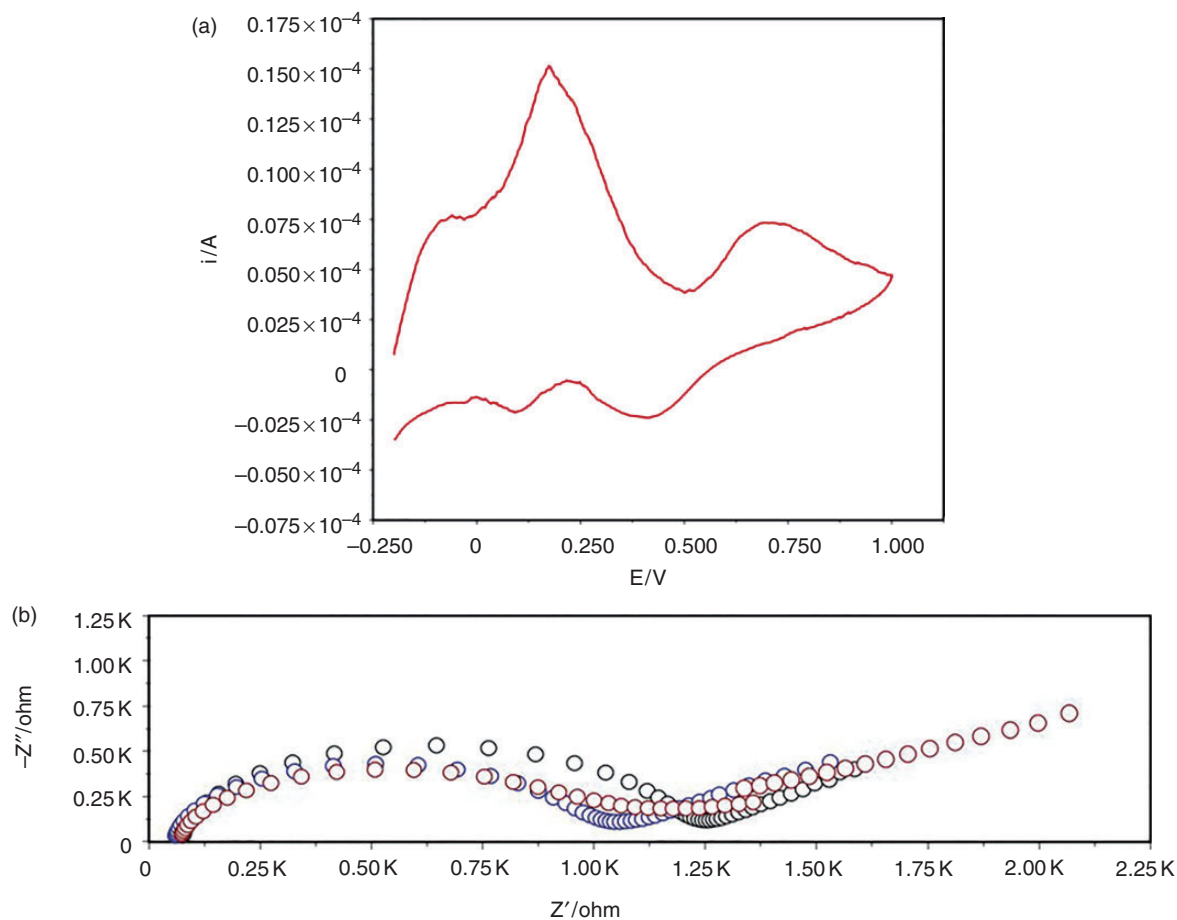


Figure 3. (a) Cyclic voltammogram and (b) electrochemical impedance spectroscopy measurement of PAN/PPy nanofibers.

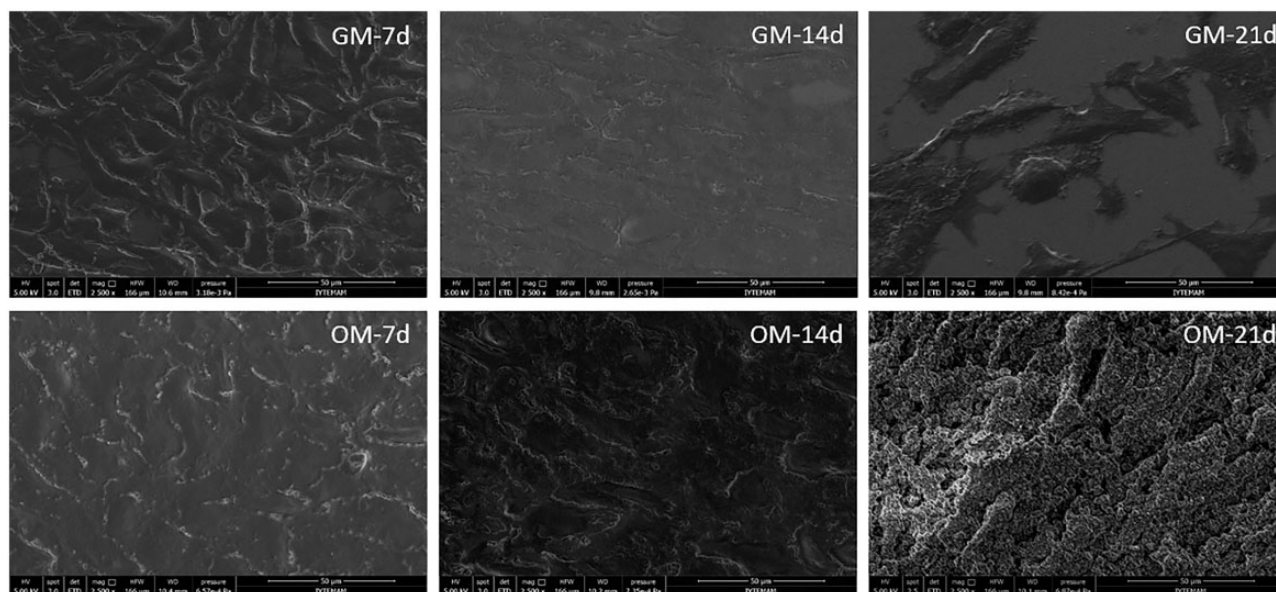


Figure 4. SEM images of MSCs after culturing in growth medium (GM) and in osteogenic medium (OM) for 7, 14, and 21 days on glass control coverslips. Scale bar is 50 μm.

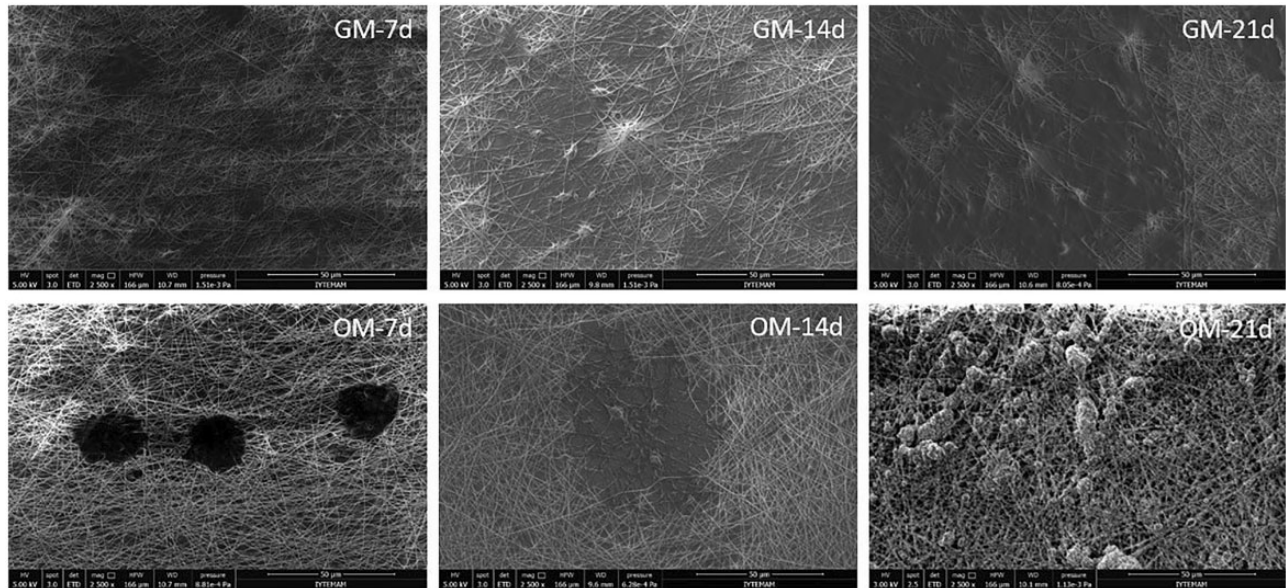


Figure 5. SEM images of MSCs after culturing in growth medium and osteogenic medium for 7, 14, and 21 days on the random PAN/PPy nanofibers (250 r/min). Scale bar is 50 μm .

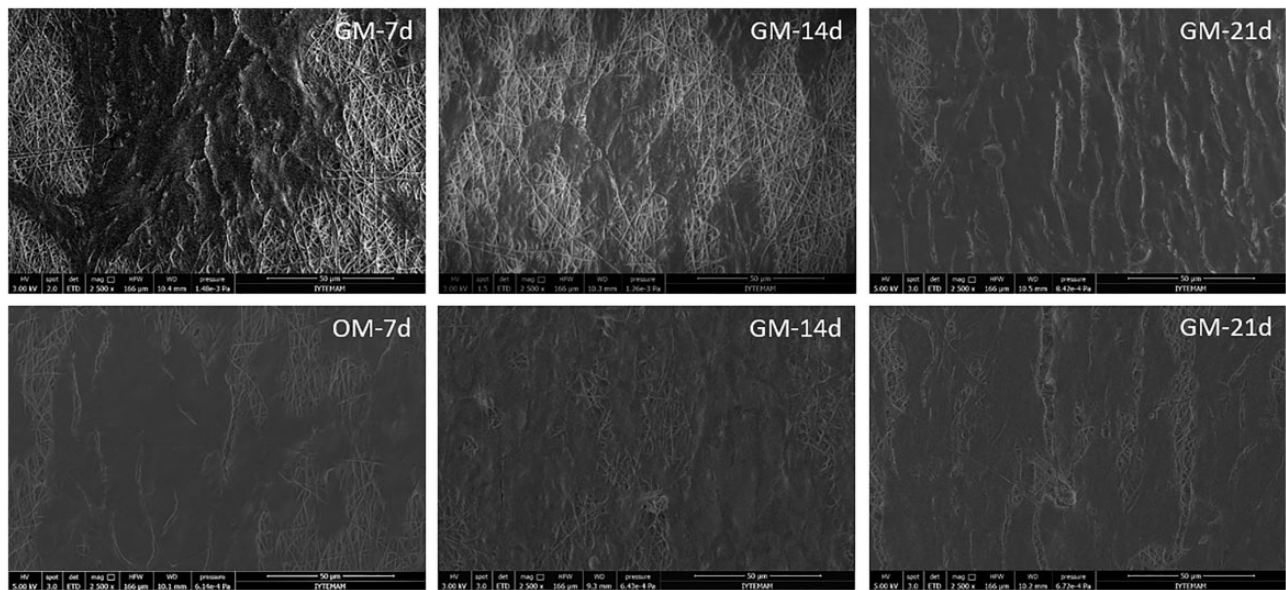


Figure 6. SEM images of MSCs after culturing in growth medium and osteogenic medium for 7, 14, and 21 days on the aligned PAN/PPy nanofibers (1000 r/min). Scale bar is 50 μm .

a cellular morphology that aligned and elongated in accordance with the fiber alignment direction (Figure 6). This observation was valid for cells grown in both quiescent and osteogenic conditions.

In order to understand the degradation behavior of PAN/PPy nanofibers in culture conditions, both random and aligned nanofibers were put into the growth and osteogenic medium without inoculation of cells for 21 days. SEM images of nanofibers

indicated that after 21 days, the morphology of fibers did not appear to change (Figure 7, Table 2).

Viability results of the D1 ORL UVA mesenchymal stem cells cultured on glass surface and PAN/PPy nanofibers showed cells were able to attach and proliferate on glass, randomly oriented and aligned PAN/PPy fibers similarly during three weeks of cell culture (Figure 8). Viability was similar for cells that were cultured in growth and osteogenic conditions, suggesting

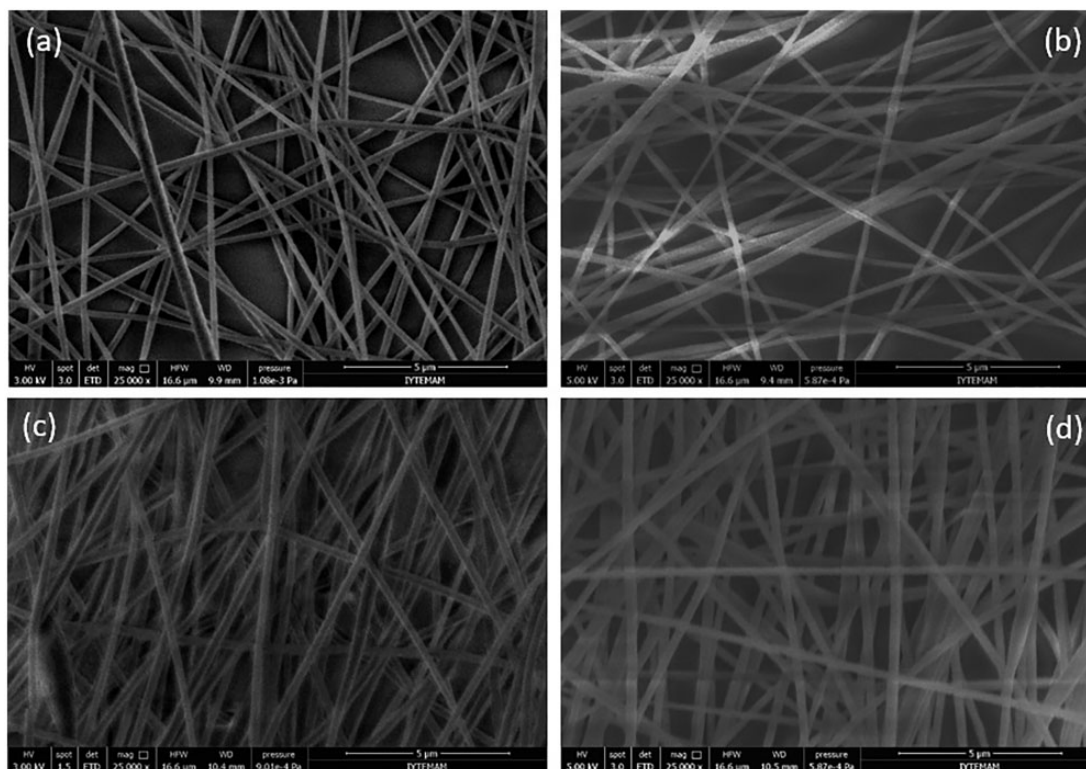


Figure 7. SEM images of random nanofibers kept in (a) GM (b) OM, and aligned nanofibers kept in (c) GM, (d) OM after 21 days.

Table 2. Average fiber diameter for random and aligned nanofibers (NFs) after keeping in OM and GM for 21 days (without cell seeding).

	Random NFs	Aligned NFs
Ave. diameter	268 (± 49)	225 (± 72)
Ave. diameter (GM)	262 (± 40)	248 (± 53)
Ave. diameter (OM)	283 (± 67)	235 (± 39)

GM: growth medium; OM: osteogenic medium.

that PAN/PPy nanofibers were nontoxic for osteoblasts and could be utilized as scaffold for osteogenic differentiation of mesenchymal stem cells. These results are consistent with previous studies, which showed that D1 cells are as viable and active in 3D scaffolds as 2D surfaces.⁵¹ MTT results, although an indirect measure of cell proliferation, concurred that PPy/PAN nanofiber scaffold was nontoxic, and cells were able to attach and grow on the scaffold, compared to the baseline values. The mineral deposition on PAN/PPy electrospun nanofibrous scaffolds was confirmed using Alizarin red staining after the 21 days of incubation period. Results indicated that D1 ORL UVA mesenchymal stem cells cultured with both 50% dose (half-dose) and 100% dose (full-dose) osteogenic media was committed to osteogenesis, while cells in growth media

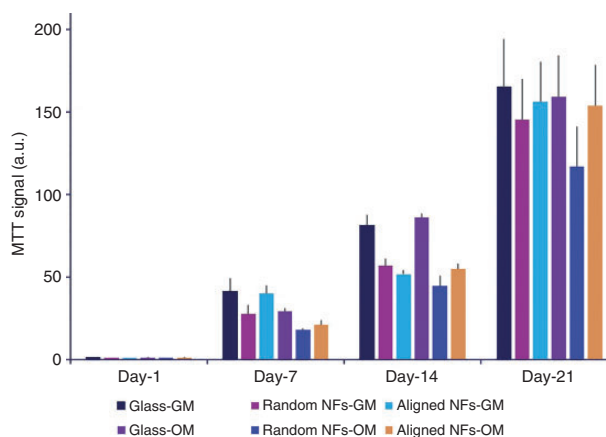


Figure 8. MTT assay of D1 ORL UVA mesenchymal stem cells on 2D glass surface or in PPy nanofiber scaffolds after 1, 7, 14, and 21 days of culture. r: randomly oriented; a: aligned; GM: growth media; OM: osteogenic media.

did not show any mineral deposition (Figure 9). However, mineral deposition observed in full-dose osteogenic media was more distinct at the end of three weeks compared to half-dose. Furthermore, oriented mineral deposition was observed in scaffolds with aligned fibers, while mineralization was randomly oriented in 2D glass culture and nonoriented fiber scaffolds. While dexamethasone was induced for osteogenesis, mineral

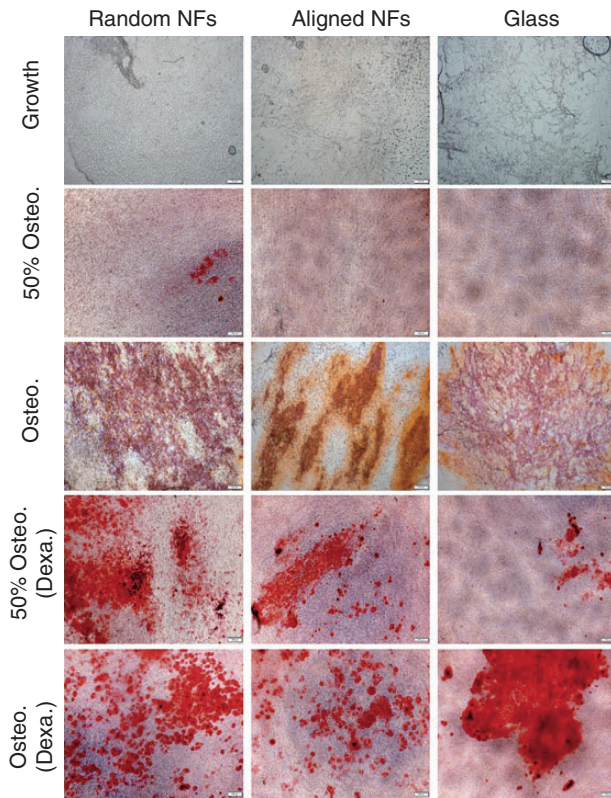


Figure 9. Alizarin red staining on random NFs, aligned NFs and glass control for growth and (50% and 100%) osteogenic conditions after 21 days. Scale bar is 200 μm .

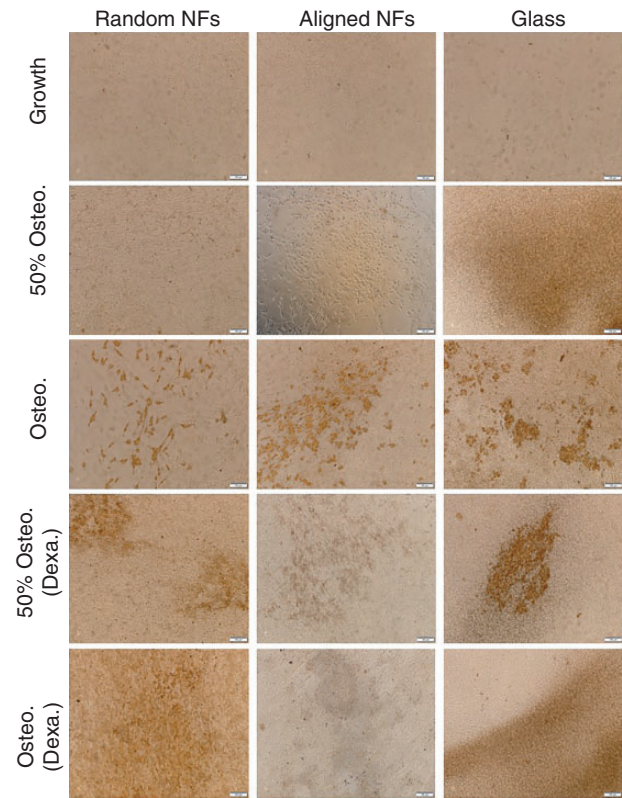


Figure 10. von Kossa staining after on random NFs, aligned NFs and glass control for growth and (50% and 100%) osteogenic conditions 21 days. Scale bar is 100 μm .

deposition increased for half-dose osteogenic media compared to β -glycerolphosphate and ascorbic acid, but there was not a significant advantage of dexamethasone in osteogenesis for full-dose. Alternative staining using von Kossa method showed similar calcification trends in control and experimental groups, consistent with Alizarin red staining (Figure 10).

PPy electrospun nanofibers were utilized with different co-polymers as tissue engineering scaffold. PPy-coated silk fibroin nanofibers indicated high electroactivity and they are used for human mesenchymal stem cells and fibroblasts culture and the results showed that silk fibroin nanofibers with their both PPy-coated and uncoated forms supported these cells attachment, spreading, and growth in vitro; however, the bioactivity of PPy-coated nanofibers was found to be low.⁵² PPy was also examined with poly(butylene adipate-co-terephthalate) (PBAT) to obtain electrically conductive electrospun nanofibers and these PBAT/PPy nanofibers were found to be a good candidate for bone tissue engineering.⁵³ PAN was also tried with PPy before; however, PAN and PPy were not blended together as done in our study, but rather PAN nanofibers were synthesized with electrospinning and then coated with PPy. These PPy-coated PAN

nanofibers were utilized as conductive scaffolds, in which nanofibers supported cell viability and the electrical stimulations improved the proliferation and accelerated neural maturation.⁵⁴ PAN/PPy electrospun nanofibers were also examined for keratinocyte culture in our previous study and their biocompatibility and suitability for keratinocytes growth were demonstrated.⁴⁸ However, this study is the first report on blended PAN/PPy nanofibers to be used for bone tissue engineering.

Similar to our application, chitosan based electrospun nanofibrous scaffolds were also studied for osteoblast-like cells.⁵⁵ While the majority of observed osteoblast-like cells were in spindle morphology, the cells were expanded on nanofibrous scaffold relatively better compared to osteoblast-like cells grown on control chitosan film. PLLA/PCL/hydroxyapatite (HAP) electrospun nanofibers were another scaffold tested for the mouse calvaria-derived pre-osteoblastic cells (MC3T3-E1). This scaffold exhibited a good attachment and proliferation of osteoblasts and differentiation was also facilitated with this scaffold.^{56,57} PVA thin layer was deposited on electrospun nylon 6 hybrid nanofibers by a hydrothermal process were found to be very effective for bone tissue

regeneration.⁵⁸ Gelatin electrospun fibrous scaffolds also supported adhesion and proliferation of osteoblasts and osteo-differentiation of mesenchymal stem cell.⁵⁹ Cross-linked boron-nitride-reinforced gelatin electrospun scaffold was examined for human bone cells and showed nontoxic and biodegradable behavior.⁶⁰ It is confirmed that PAN/PPy is a suitable to use as a bone tissue engineering scaffold with its mineralization ability. Generally, many polymeric materials including natural and synthetic polymers in their fiber form have been developed for bone tissue engineering.¹ However, the crucial thing is to find a scaffold supporting the adhesion, proliferation and differentiation of mesenchymal stem cells for bone tissue engineering. In this study, PAN/PPy nanofibers as a new material for osteogenic differentiation of mesenchymal stem cells with their random and aligned forms supported osteogenic differentiation of mesenchymal stem cells and indicated good viability for osteoblasts. Therefore PAN/PPy nanofibers may find a suitable application in bone tissue engineering era such as in the repair of bone defects, periosteum and reconstruction.^{61,62}

Scaffold mechanical properties and cell–cell interaction are two significant parameters that regulate osteogenic differentiation of mesenchymal stem cells.⁶³ Our results also suggested that mechanical properties of the scaffold played a major role in cell viability as cell viability on aligned nanofibers, which indicated higher strength, were higher than random nanofibers.

Conclusions

We investigated random and aligned PAN/PPy nanofibers as scaffold for osteogenic differentiation of mesenchymal stem cells. These electrospun nanofibers were found to be biocompatible for osteoblast growth and supported differentiation of mesenchymal stem cells. Cell attachment and proliferation were observed for mesenchymal stem cells and their differentiated form. The cells on random nanofibers showed a tendency of creating groups and getting together on the randomly oriented nanofibrous scaffold, whereas the cells appeared to align and elongate in the major fiber direction when they were seeded on aligned nanofibers. Alignment of nanofibers allowed to obtain an anisotropic cellular structure. MTT assay indicated that PAN/PPy nanofibers were non-toxic and Alizarin red and Von Kossa assays showed that osteogenesis was induced on mesenchymal stem cells osteogenesis on these nanofibers.

Declaration of conflicting interests

The author(s) declared no potential conflicts of interest with respect to the research, authorship, and/or publication of this article.

Funding

The author(s) received no financial support for the research, authorship, and/or publication of this article.

ORCID iD

Atike Ince Yardimci  <https://orcid.org/0000-0001-5482-4230>

References

- Ladd MR, Hill TK, Yoo JJ, et al. Electrospun nanofibers in tissue engineering. In: *Nanofibers-production, properties and functional applications*. InTechOpen, 2011.
- Yang S, Leong K-F, Du Z, et al. The design of scaffolds for use in tissue engineering. Part I. Traditional factors. *Tissue Eng* 2001; 7: 679–689.
- Pham QP, Sharma U and Mikos AG. Electrospinning of polymeric nanofibers for tissue engineering applications: a review. *Tissue Eng* 2006; 12: 1197–1211.
- Ju YM, San Choi J, Atala A, et al. Bilayered scaffold for engineering cellularized blood vessels. *Biomaterials* 2010; 31: 4313–4321.
- Liu H, Ding X, Zhou G, et al. Electrospinning of nanofibers for tissue engineering applications. *J Nanomater* 2013; 2013: 3.
- Flemming R, Murphy C, Abrams G, et al. Effects of synthetic micro-and nano-structured surfaces on cell behavior. *Biomaterials* 1999; 20: 573–588.
- Sheridan RL, Morgan JR, Cusick JL, et al. Initial experience with a composite autologous skin substitute. *Burns* 2001; 27: 421–424.
- Huang Z-M, Zhang Y-Z, Kotaki M, et al. A review on polymer nanofibers by electrospinning and their applications in nanocomposites. *Compos Sci Technol* 2003; 63: 2223–2253.
- Thavasi V, Singh G and Ramakrishna S. Electrospun nanofibers in energy and environmental applications. *Energy Environ Sci* 2008; 1: 205–221.
- Fang J, Niu H, Lin T, et al. Applications of electrospun nanofibers. *Chinese Sci Bull* 2008; 53: 2265.
- Oliveira MF, Suarez D, Rocha JCB, et al. Electrospun nanofibers of polyCD/PMAA polymers and their potential application as drug delivery system. *Mater Sci Eng C* 2015; 54: 252–261.
- Potrč T, Baumgartner S, Roškar R, et al. Electrospun polycaprolactone nanofibers as a potential oromucosal delivery system for poorly water-soluble drugs. *Eur J Pharmaceut Sci* 2015; 75: 101–113.
- Wang X, Yu D-G, Li X-Y, et al. Electrospun medicated shellac nanofibers for colon-targeted drug delivery. *Int J Pharmaceut* 2015; 490: 384–390.
- Aytac Z, Sen HS, Durgun E, et al. Sulfoxazole/cyclodextrin inclusion complex incorporated in electrospun

- hydroxypropyl cellulose nanofibers as drug delivery system. *Colloids Surf B* 2015; 128: 331–338.
15. Nur-E-Kamal A, Ahmed I, Kamal J, et al. Three dimensional nanofibrillar surfaces induce activation of Rac. *Biochem Biophys Res Commun* 2005; 331: 428–434.
 16. Kennedy KM, Bhaw-Luximon A and Jhurry D. Cell-matrix mechanical interaction in electrospun polymeric scaffolds for tissue engineering: Implications for scaffold design and performance. *Acta Biomater* 2017; 50: 41–55.
 17. Nerurkar NL, Elliott DM and Mauck RL. Mechanics of oriented electrospun nanofibrous scaffolds for annulus fibrosus tissue engineering. *J Orthop Res* 2007; 25: 1018–1028.
 18. Ghasemi-Mobarakeh L, Prabhakaran MP, Morshed M, et al. Electrospun poly (ϵ -caprolactone)/gelatin nanofibrous scaffolds for nerve tissue engineering. *Biomaterials* 2008; 29: 4532–4539.
 19. Xu C, Inai R, Kotaki M, et al. Aligned biodegradable nanofibrous structure: a potential scaffold for blood vessel engineering. *Biomaterials* 2004; 25: 877–886.
 20. Fan Z, Swadener J, Rho J, et al. Anisotropic properties of human tibial cortical bone as measured by nanoindentation. *J Orthop Res* 2002; 20: 806–810.
 21. Abdel-Wahab AA, Alam K and Silberschmidt VV. Analysis of anisotropic viscoelastoplastic properties of cortical bone tissues. *J Mech Behav Biomed Mater* 2011; 4: 807–820.
 22. Guo Z, Xu J, Ding S, et al. In vitro evaluation of random and aligned polycaprolactone/gelatin fibers via electrospinning for bone tissue engineering. *J Biomater Sci Polym Ed* 2015; 26: 989–1001.
 23. Meng Z, Wang Y, Ma C, et al. Electrospinning of PLGA/gelatin randomly-oriented and aligned nanofibers as potential scaffold in tissue engineering. *Mater Sci Eng C* 2010; 30: 1204–1210.
 24. McCullen SD, Autefage H, Callanan A, et al. Anisotropic fibrous scaffolds for articular cartilage regeneration. *Tissue Eng A* 2012; 18: 2073–2083.
 25. Lakard S, Herlem G, Propper A, et al. Adhesion and proliferation of cells on new polymers modified biomaterials. *Bioelectrochemistry* 2004; 62: 19–27.
 26. Stauffer WR and Cui XT. Polypyrrole doped with 2 peptide sequences from laminin. *Biomaterials* 2006; 27: 2405–2413.
 27. Garner B, Hodgson A, Wallace G, et al. Human endothelial cell a. *J Mater Sci: Mater Med* 1999; 10: 19–27.
 28. Ateh DD, Vadgama P and Navsaria HA. Culture of human keratinocytes on polypyrrole-based conducting polymers. *Tissue Eng* 2006; 12: 645–655.
 29. Gilmore KJ, Kita M, Han Y, et al. Skeletal muscle cell proliferation and differentiation on polypyrrole substrates doped with extracellular matrix components. *Biomaterials* 2009; 30: 5292–5304.
 30. Lee JY, Bashur CA, Goldstein AS, et al. Polypyrrole-coated electrospun PLGA nanofibers for neural tissue applications. *Biomaterials* 2009; 30: 4325–4335.
 31. Bechara S, Wadman L and Papat KC. Electroconductive polymeric nanowire templates facilitates in vitro C17. 2 neural stem cell line adhesion, proliferation and differentiation. *Acta Biomater* 2011; 7: 2892–2901.
 32. Castano H, O'Rear EA, McFetridge PS, et al. Polypyrrole thin films formed by admicellar polymerization support the osteogenic differentiation of mesenchymal stem cells. *Macromol Biosci* 2004; 4: 785–794.
 33. Li X, Hao X, Yu H, et al. Fabrication of polyacrylonitrile/polypyrrole (PAN/Ppy) composite nanofibres and nanospheres with core-shell structures by electrospinning. *Mater Lett* 2008; 62: 1155–1158.
 34. Baskan O, Mese G and Ozcivici E. Low-intensity vibrations normalize adipogenesis-induced morphological and molecular changes of adult mesenchymal stem cells. *Proc IMechE, Part H: J Engineering Medicine* 2017; 231: 160–168.
 35. Demiray L and Özçivici E. Bone marrow stem cells adapt to low-magnitude vibrations by altering their cytoskeleton during quiescence and osteogenesis. *Turkish J Biol* 2015; 39: 88–97.
 36. Jin G, He R, Sha B, et al. Electrospun three-dimensional aligned nanofibrous scaffolds for tissue engineering. *Mater Sci Eng C* 2018; 92: 995–1005.
 37. Aviss K, Gough J and Downes S. Aligned electrospun polymer fibres for skeletal muscle regeneration. *Eur Cell Mater* 2010; 19: 193–204.
 38. Wang W, Caetano G, Ambler WS, et al. Enhancing the hydrophilicity and cell attachment of 3D printed PCL/graphene scaffolds for bone tissue engineering. *Materials* 2016; 9: 992.
 39. Moffat KL, Kwei A-P, Spalazzi JP, et al. Novel nanofiber-based scaffold for rotator cuff repair and augmentation. *Tissue Eng A* 2008; 15: 115–126.
 40. Baker BM, Nerurkar NL, Burdick JA, et al. Fabrication and modeling of dynamic multipolymer nanofibrous scaffolds. *J Biomech Eng* 2009; 131: 101012.
 41. Xie J, Li X, Lipner J, et al. Aligned-to-random nanofiber scaffolds for mimicking the structure of the tendon-to-bone insertion site. *Nanoscale* 2010; 2: 923–926.
 42. Fan X, Rahnert JA, Murphy TC, et al. Response to mechanical strain in an immortalized pre-osteoblast cell is dependent on ERK1/2. *J Cell Physiol* 2006; 207: 454–460.
 43. Robling AG, Castillo AB and Turner CH. Biomechanical and molecular regulation of bone remodeling. *Annu Rev Biomed Eng* 2006; 8: 455–498.
 44. Wozniak M, Fausto A, Carron CP, et al. Mechanically strained cells of the osteoblast lineage organize their extracellular matrix through unique sites of $\alpha V\beta 3$ -integrin expression. *J Bone Miner Res* 2000; 15: 1731–1745.
 45. Simmons CA, Matlis S, Thornton AJ, et al. Cyclic strain enhances matrix mineralization by adult human mesenchymal stem cells via the extracellular signal-regulated kinase (ERK1/2) signaling pathway. *J Biomech* 2003; 36: 1087–1096.
 46. Kestenbach H-J and Rogausch K-D. Molecular orientation of individual LCP particles in injection-moulded PPS/LCP blends. *Mater Res* 2003; 6: 75–83.
 47. Nobeshima T, Sakai H, Ishii Y, et al. Polarized FT-IR study of uniaxially aligned electrospun poly (DL-lactic acid) fiber films. *J Photopol Sci Technol* 2016; 29: 353–356.

48. Ince Yardimci A, Aypek H, Ozturk O, et al. CNT incorporated polyacrylonitrile/polypyrrole nanofibers as keratinocytes scaffold. *J Biomim Biomater Biomed Eng* 2019; 41: 69–81.
49. Yanilmaz M and Zhang X. Polymethylmethacrylate/polyacrylonitrile membranes via centrifugal spinning as separator in Li-ion batteries. *Polymers* 2015; 7: 629–643.
50. Anil-Inevi M, Yaman S, Yildiz AA, et al. Biofabrication of in situ self-assembled 3D cell cultures in a weightlessness environment generated using magnetic levitation. *Scient Rep* 2018; 8: 7239.
51. Karadas O, Mese G and Ozcivici E. Cytotoxic tolerance of healthy and cancerous bone cells to anti-microbial phenolic compounds depend on culture conditions. *Appl Biochem Biotechnol* 2019; 188: 514–526.
52. Aznar-Cervantes S, Roca MI, Martinez JG, et al. Fabrication of conductive electrospun silk fibroin scaffolds by coating with polypyrrole for biomedical applications. *Bioelectrochemistry* 2012; 85: 36–43.
53. de Castro JG, Rodrigues BV, Ricci R, et al. Designing a novel nanocomposite for bone tissue engineering using electrospun conductive PBAT/polypyrrole as a scaffold to direct nanohydroxyapatite electrodeposition. *RSC Adv* 2016; 6: 32615–32623.
54. Xu Q, Jin L, Li C, et al. The effect of electrical stimulation on cortical cells in 3D nanofibrous scaffolds. *RSC Adv* 2018; 8: 11027–11035.
55. Sangsanoh P, Suwanton O, Neamark A, et al. In vitro biocompatibility of electrospun and solvent-cast chitosan substrata towards Schwann, osteoblast, keratinocyte and fibroblast cells. *Eur Polym J* 2010; 46: 428–440.
56. Jaiswal A, Chhabra H, Soni V, et al. Enhanced mechanical strength and biocompatibility of electrospun polycaprolactone-gelatin scaffold with surface deposited nano-hydroxyapatite. *Mater Sci Eng C Mater Biol Appl* 2013; 33: 2376–2385.
57. Qi H, Ye Z, Ren H, et al. Bioactivity assessment of PLLA/PCL/HAP electrospun nanofibrous scaffolds for bone tissue engineering. *Life Sci* 2016; 148: 139–144.
58. Abdal-Hay A, Hamdy AS and Khalil KA. Fabrication of durable high performance hybrid nanofiber scaffolds for bone tissue regeneration using a novel, simple in situ deposition approach of polyvinyl alcohol on electrospun nylon 6 nanofibers. *Mater Lett* 2015; 147: 25–28.
59. Lin W-H, Yu J, Chen G, et al. Fabrication of multi-biofunctional gelatin-based electrospun fibrous scaffolds for enhancement of osteogenesis of mesenchymal stem cells. *Colloids Surf B* 2016; 138: 26–31.
60. Nagarajan S, Belaid H, Pochat-Bohatier C, et al. Design of boron nitride/gelatin electrospun nanofibers for bone tissue engineering. *ACS Appl Mater Interfaces* 2017; 9: 33695–33706.
61. Lyu S, Huang C, Yang H, et al. Electrospun fibers as a scaffolding platform for bone tissue repair. *J Orthop Res* 2013; 31: 1382–1389.
62. McMahan RE, Wang L, Skoracki R, et al. Development of nanomaterials for bone repair and regeneration. *J Biomed Mater Res* 2013; 101: 387–397.
63. Mao AS, Shin J-W and Mooney DJ. Effects of substrate stiffness and cell-cell contact on mesenchymal stem cell differentiation. *Biomaterials* 2016; 98: 184–191.